Magnetization Transfer MR of the Normal Adult Brain

Rahul C. Mehta, G. Bruce Pike, and Dieter R. Enzmann

PURPOSE: To establish a normal baseline of the percent magnetization transfer of gray (cortical and deep) and white matter structures in the brain in healthy adults and to determine whether there are adult age-related differences in these measurements. **METHODS:** Axial T1-weighted scans (800/20 [repetition time/echo time]) with and without magnetization transfer were prospectively performed on a 1.5-T MR imaging unit on 68 healthy patients (aged 20 to 76 years). Presaturation and postsaturation magnetization transfer images were obtained using an on-resonance binomial pulse. All patients had normal MR scans on all pulse sequences. A calculated "difference" image was used to calculate the percent magnetization transfer in multiple specific regions of the brain. In each hemisphere, 9 discrete areas of cortical and deep gray matter and 29 areas of white matter were measured in 68 patients to generate age-related changes in percent magnetization transfer in these anatomic regions. Ranges of normal percent magnetization transfer in each of the 38 measures were established. **RESULTS:** The percent magnetization transfer of the gray matter (28% ± 2%) was lower than that of the white matter (36% ± 2%). There was no statistically significant difference in the percent magnetization transfer in different areas of gray matter. Deep white matter in the different lobes (percent magnetization transfer, 31% to 38%) also showed no differences by age. Percent magnetization transfer was the highest in the genu of the corpus callosum (42%), and this was statistically significant compared with other white matter measurements. **CONCLUSION:** There were no statistically significant age-related variations in the percent magnetization transfer in healthy adults in gray or white matter. These percent magnetization transfer measurements provide baseline normative data, which can be used to measure the extent and severity of white matter changes in disease states.

Index terms: Brain, anatomy; Magnetic resonance, magnetization transfer

AJNR Am J Neuroradiol 16:2085–2091, November 1995

Magnetic resonance (MR) is dominated by the contribution of freely mobile water protons because of their great abundance and their sharp resonance frequency. Nevertheless, relaxation of water protons by interactions with macromolecular protons found in proteins and cellular membranes does contribute to the signal derived in proton MR. The protons in macromolecular proteins have restricted motion, and they interact with mobile water protons through coupling and chemical exchange. Exchange of magnetization between highly mobile, free water protons and immobile, restricted water protons, is a primary mechanism for spin lattice (T1) relaxation in tissues (1–4).

Wolff and Balaban (2) have described a new form of tissue contrast: magnetization transfer contrast. The exchange of magnetization in tissues after a saturating pulse is determined by the relative proportion of the two pools of hydrogen atoms: a highly mobile ("free") hydrogen pool, H_f, and an immobile ("restricted") hydrogen pool, H_r, the latter being those protons bound to large macromolecular protein molecules such as those found in cellular membranes. Thus the presence of the restricted pool can be detected by imaging the free pool of protons. The H_f have a discrete and a sharp central peak on MR spectroscopy, and the H_r have a "broad" spectrum disposed symmetrically around the H_f peak. Direct observation of

Received December 5, 1994; accepted after revision May 31, 1995.

From the Department of Radiology, Stanford (Calif) University School of Medicine.

Address reprint requests to Dieter R. Enzmann, MD, Department of Radiology, 5047, Stanford University School of Medicine, Stanford, CA 94305-5105.

AJNR 16:2085–2091, Nov 1995 0195-6108/95/1610–2085

TABLE 1: Magnetization transfer (%, mean ± SEM) in the age groups, for the different regions of the white matter

	Age, y					
	21–30	31–40	41–50	51–60	61–70	71–80
Central Corpus	36.00 ± 0.7	36.80 ± 0.4	38.20 ± 0.5	39.40 ± 0.5	39.00 ± 0.5	39.40 ± 0.8
Peri Corpus	35.50 ± 1.0	34.50 ± 0.7	34.70 ± 0.8	35.90 ± 0.7	35.30 ± 0.7	36.60 ± 0.8
Brachium Pontis	34.20 ± 0.4	36.30 ± 0.6	38.10 ± 0.9	38.80 ± 1.4	38.60 ± 0.6	37.80 ± 1.5
Tectum	34.90 ± 0.2	35.90 ± 0.5	36.90 ± 0.4	37.30 ± 0.8	38.00 ± 0.4	37.80 ± 0.4
Tegmentum	33.20 ± 0.6	33.10 ± 0.6	34.80 ± 0.9	35.00 ± 1.0	35.60 ± 0.5	35.80 ± 0.8
Optic Tract	33.20 ± 0.6	32.60 ± 0.6	34.40 ± 0.6	33.90 ± 0.9	34.10 ± 0.6	34.80 ± 0.7
Peduncle-Med	32.90 ± 0.7	35.20 ± 0.7	35.80 ± 0.7	36.30 ± 0.8	37.20 ± 0.7	35.30 ± 0.7
Peduncle-Lat	34.00 ± 0.7	35.50 ± 0.5	36.10 ± 0.5	37.50 ± 0.6	37.50 ± 0.5	35.20 ± 1.1
Frontal L Central	35.60 ± 0.6	36.60 ± 0.5	37.80 ± 0.7	37.50 ± 0.6	37.30 ± 0.6	36.80 ± 1.0
Frontal L U Fiber	33.20 ± 0.8	33.90 ± 0.5	34.00 ± 0.6	34.00 ± 1.1	34.70 ± 0.6	34.40 ± 1.2
Parietel L Central	33.60 ± 0.4	34.60 ± 0.5	35.10 ± 1.0	34.50 ± 0.6	37.00 ± 1.0	36.90 ± 1.0
Parietel L U Fiber	31.30 ± 0.6	31.70 ± 0.6	32.40 ± 1.0	31.40 ± 0.7	33.30 ± 0.9	33.00 ± 0.6
Temporal L Central	37.40 ± 1.2	38.20 ± 0.3	38.60 ± 0.4	39.10 ± 0.5	37.80 ± 0.5	37.80 ± 1.1
Temporal L U Fiber	34.40 ± 0.6	34.70 ± 0.5	34.30 ± 0.6	36.10 ± 0.5	34.70 ± 0.6	33.50 ± 1.1
Optic Radiations	37.60 ± 0.1	37.20 ± 0.3	37.30 ± 0.3	37.60 ± 0.2	37.10 ± 0.6	37.90 ± 0.4
Occipital L Central	38.50 ± 0.2	38.20 ± 0.2	38.70 ± 0.3	39.40 ± 0.5	37.90 ± 0.5	39.40 ± 0.4
Occipital L U Fiber	34.60 ± 0.7	35.70 ± 0.3	36.00 ± 0.6	34.40 ± 0.8	36.10 ± 0.5	36.60 ± 1.1
IC-Ant	34.30 ± 0.4	34.30 ± 0.3	34.20 ± 0.4	33.80 ± 0.6	34.70 ± 0.5	35.10 ± 0.9
IC-Genu	36.20 ± 0.4	36.30 ± 0.3	36.10 ± 0.4	35.80 ± 0.5	36.50 ± 0.3	36.50 ± 0.6
IC-Post	38.40 ± 0.4	38.10 ± 0.3	36.10 ± 0.5	35.80 ± 0.7	38.90 ± 0.5	39.60 ± 0.7
External Capsule	32.80 ± 0.9	30.40 ± 0.4	31.90 ± 0.9	33.60 ± 0.5	33.30 ± 0.6	33.60 ± 1.1
CC-Genu	41.10 ± 0.4	40.70 ± 0.3	40.70 ± 0.5	41.50 ± 0.5	41.70 ± 0.4	41.00 ± 0.7
CC-Splenium	36.90 ± 0.7	37.70 ± 0.3	37.50 ± 0.4	38.00 ± 0.4	38.90 ± 0.6	37.50 ± 0.5
Fornix	30.60 ± 1.2	30.40 ± 0.7	32.00 ± 1.0	32.10 ± 0.8	32.10 ± 0.5	31.10 ± 0.7
Centrum Semiovale	38.40 ± 0.2	38.10 ± 0.2	38.20 ± 0.3	38.30 ± 0.2	39.30 ± 0.7	39.50 ± 0.8
Fasciculus SFO	37.10 ± 0.3	37.10 ± 0.3	37.00 ± 0.3	36.90 ± 0.4	36.40 ± 0.6	38.00 ± 0.6
Centrum U Fiber	34.90 ± 0.2	34.80 ± 0.3	35.80 ± 0.5	35.10 ± 0.3	35.10 ± 0.2	35.60 ± 0.7
Cingulum	35.30 ± 0.9	34.90 ± 0.6	34.80 ± 0.9	33.70 ± 1.2	36.20 ± 0.7	35.60 ± 1.2
Ant Comm	30.00 ± 1.3	29.90 ± 0.7	28.90 ± 0.8	29.30 ± 0.8	29.30 ± 0.6	31.20 ± 0.7

Note.—Peri corpus indicates peripheral white matter of the corpus medullaris; peduncle-med and peduncle-lat, medial and lateral cerebral peduncles; IC-ant, IC-genu, and IC-post, internal capsule, anterior limb, genu, and posterior limb, respectively; CC-genu and CC-splenium, corpus callosum genu and splenium; fasciculus SFO, superior frontooccipital fasciculus; and ant comm, anterior commissure.

the H_r magnetization pool is normally not possible because of its extremely short T2 (<200 microseconds). However, saturation of the restricted pool will have a detectable effect on the free-proton pool. This effect is one of decreasing the signal of the free pool by transferring the restricted pool's saturation. The rate of magnetization transfer is determined by the relative proportion of the two pools of hydrogen atoms, their efficiency of interaction, the field strength, and scanning parameters.

Findings in preliminary studies have demonstrated that the magnetization transfer technique may be useful in several cranial imaging applications: for improved detection of intracranial central nervous system lesions (5–13), for improving small-vessel delineation at time-of-flight MR angiography (14–19), for increasing tissue contrast in gradient-echo imaging (20, 21), for characterizing and assessing the age of multiple sclerosis lesions (22, 23), for evaluating cerebral ischemia and infarction (24–26), for evaluating the cervical spine (27), knee (28), heart, and coronary vessels (29, 30), and for detecting wallerian degeneration (31).

As magnetization transfer techniques become more widely disseminated and used for general diagnostic purposes, it becomes increasingly important to have a normal baseline available for image and measurement interpretation. A previously published study has described new patterns of tissue contrast and the increased visibility of normally enhancing structures (32). The purpose of our study was to establish a quantitative range of normal of percent magnetization transfer in different tissues in the normal brain and to determine whether there is an adult age-related change in the percent magnetization transfer in the various gray and white matter structures.

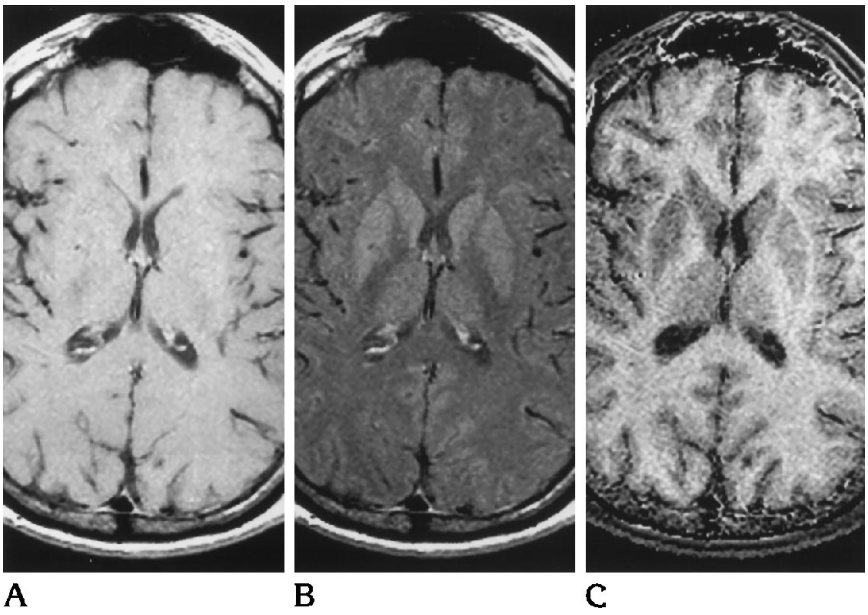

Fig 1. A 55-year-old healthy subject.

A, Axial T1-weighted image without magnetization transfer; *B*, axial T1-weighted image with magnetization transfer; and *C*, difference image at the level of the basal ganglia and the thalamus. On *B* there is a suppression of the white matter signal in the anterioposterior limb and the genu of the internal capsule, the external capsule, and the subcortical and deep periventricular white matter. The thalamus is more suppressed on *B* than the caudate nucleus, the putamen, and the cortex. Note that the thalamus is the most hyperintense cortical or deep periventricular gray matter structure in the brain.

Materials and Methods

This study was performed prospectively over a 4-month period and involved 68 adults (ages 21 to 78 years). The patients were grouped by age as follows: (*a*) 21 to 30 years, n = 10; (*b*) 31 to 40 years, n = 19; (*c*) 41 to 50 years; n = 11; (*d*) 51 to 60 years, n = 6; (*e*) 61 to 70 years, n = 15; and (*f*) 71 to 80 years, n = 7. The entry criteria for healthy patients was a normal MR scan on all pulse sequences including postcontrast scans. A review of the medical history of each patient was performed to exclude any patients with central nervous system disorders or systemic disease, which would preclude inclusion in this study. The detection of any abnormality resulted in exclusion. These patients had histories of single isolated complaints, and the MR was obtained to rule out structural abnormalities. The work-up ceased with a negative MR. Patients with chronic symptoms and unresolved diagnosis were not included. All the studies were performed on a General Electric 1.5-T Signa MR imaging unit (General Electric, Milwaukee, Wis) using a head coil and 18- to 24-cm field of view. The brain MR protocol was as follows: (*a*) sagittal T1-weighted, 800/20/1 (repetition time/echo time/excitations), 5-mm sections with 2.5-mm intersection spacing; (*b*) axial T2-weighted, 2000/30,80/2, 4-mm sections with 1.0-mm intersection spacing; (*c*) axial precontrast T1-weighted, with and without magnetization transfer, 800/20/1, 5-mm sections with 1.0-mm intersection spacing; and (*d*) axial postcontrast (if performed) T1-weighted with and without magnetization transfer, 800/20/1, 5-mm sections with 1.0-mm intersection spacing. All the patients signed a written consent form allowing performance of the additional magnetization transfer sequence. For magnetization transfer images, only the saturation pulse was added; the other parameters were identical (4). The specific absorption rate for the magnetization transfer sequence was well below the Food and Drug Administration limits; average specific absorption rate was 0.04 W/kg, and peak specific absorption rate was 2.53 W/kg for any gram of cranial tissue.

Magnetization transfer was performed with an on-resonance zero-degree binomial pulse to saturate the H_r pool (33, 34). This pulse has a broad pass band with no significant saturation of H_f and is reasonably insensitive to the B_0 inhomogeneities. After testing a variety of binomial pulses, the 1-2-1 pulse was found to be the best compromise between H_r saturation and H_f bandwidth (33). The main advantage of the on-resonance saturation pulse is that it is shorter, and therefore more sections can be obtained within a given time interval. It is also insensitive to B_0 inhomogeneities, and the power deposition is also less (33). A single binomial pulse is applied before each section-selective excitation in our multisection spin-echo sequence.

A total of 78 region-of-interest measurements were performed in each patient, 38 in each hemisphere and additional measurements in air and ventricles (Table 1). Nine gray matter regions were measured: cerebellum, temporal lobe, frontal lobe, parietal lobe, occipital lobe, caudate nucleus, globus pallidus, putamen, and thalamus. The white matter areas measured were corpus medullaris (central and peripheral); brachium pontis; tectum and tegmentum of the pons; optic tracts; cerebral peduncles (medial and lateral); central and subcortical (U) fibers of the temporal, frontal, parietal, and occipital lobes; optic radiations; anterior limb, genu, and posterior limb of internal capsule; external capsule; genu and splenium of the corpus callosum; fornix; centrum semiovale (central and subcortical fibers); superior frontooccipital fasciculus; cingulum; and anterior commissure.

All measurements were made by one author (R.C.M.) on an independent console using the region-of-interest function. Before the initiation of the study and on the first 15 patients a training session was undertaken by two au-

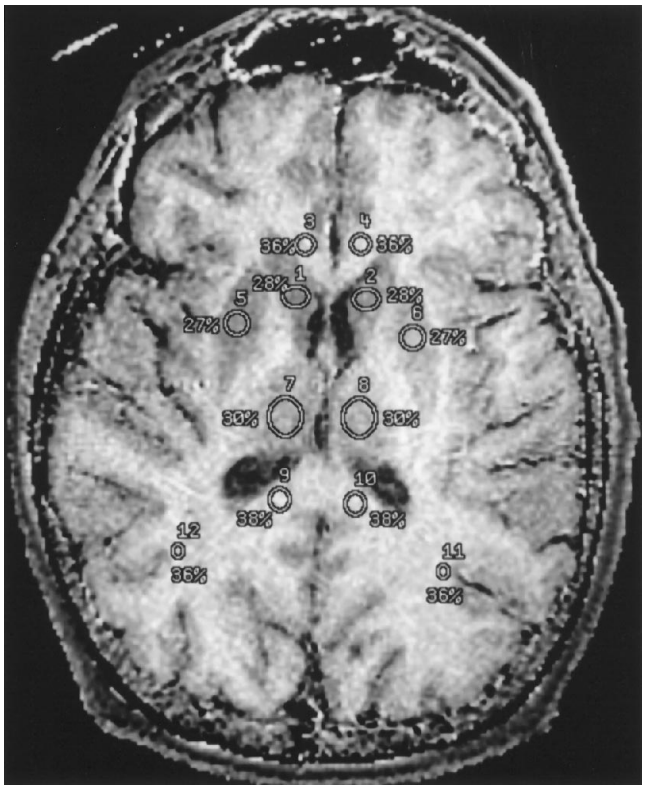

Fig 2. Magnetization transfer difference image with region-of-interest values from different gray and white matter regions in both hemispheres.

thors (R.C.M. and D.R.E.) to ensure anatomically accurate localization and consistency in the measurement technique. Once the anatomic sites were consistently located and yielded consistent measurements by both observers, R.C.M., using the consensus techniques, made all the measurements to ensure consistency. The large number of measurements per patient made this the practical approach once agreement was reached. In large gray and white matter regions reliable measurements were expected, because little partial volume (ie, gray and white matter) error was anticipated. The areas such as subcortical white matter were more susceptible to this type of variation, but it would be reflected in the SEM. The low SEMs confirm the consistency of the measurement technique.

This "difference image" was generated by subtracting the signal intensity before and after the magnetization transfer pulse and expressing the new image as percent change from baseline (non–magnetization transfer image) (Fig 1). Percent magnetization transfer was calculated by drawing circular regions of interest measuring 0.5 mm^2 and 25 mm^2 outlining an area in each of the above-mentioned regions on the calculated difference image (Fig 2). Higher signal on this image means a greater change of magnetization transfer. Identical regions of interest were chosen in the contralateral hemisphere. T1- and T2-weighted images were used for accurate anatomic location of the above-mentioned gray and white matter structures. Caution was exercised to avoid inadvertent partial voluming of other anatomic structures. Background noise was measured as the signal intensity of air (in a region not contaminated by the phase-encode artifact) and divided by the square-root of π (35). The mean, SD, and SEM were calculated for each region for each of the above-designated age groups. The measurements in various categories were compared, and tests for statistical significance (two-tailed t test) were applied.

Results

White Matter

The degree of suppression of the white matter was uniform, and there was no statistical variation in the pulse sequence during the period of the study; that is, for the adult brain, the degree of saturation of the white matter by the magnetization transfer pulse was constant throughout the study, without any significant variation. The percent magnetization transfer of various white matter anatomic structures for different age categories is shown in Table 1. The percent magnetization transfer was higher in all the white matter structures (36% $\pm$ 2%) than the gray matter (28% $\pm$ 2%), as expected ($P < .01$). The genu of the corpus callosum had the highest percent magnetization transfer, 42% ($P < .001$). There was no statistical difference in the measurements of normal white matter structures between different age groups. There was also no significant variation in the measurements between the left and right hemispheres. The range of SD and SEM was also similar for all the different locations.

The range of percent magnetization transfer of central corpus medullaris was, for all age categories, similar to that of the white matter of different lobes of the cerebrum. The peripheral corpus medullaris and the subcortical U fibers showed a slightly, but statistically not significant, lower percent magnetization transfer, probably reflecting the less-dense white matter. In the pons, the percent magnetization transfer of the tectum was slightly higher than that of the tegmentum, but this was not statistically significant ($P < .05$) (Table 1). The percent magnetization transfer of the latter may have been lower because of the presence of gray matter nuclei.

The genu of the corpus callosum had the highest percent magnetization transfer in the brain, and this was statistically significant com-

TABLE 2: Magnetization transfer (%, mean ± SEM) in the age groups of the different regions of the cortical and deep gray matter

	Age, y					
	21–30	31–40	41–50	51–60	61–70	71–80
Cerebellum	26.00 ± 0.6	27.10 ± 0.3	27.80 ± 0.6	29.00 ± 0.7	28.20 ± 1.0	39.60 ± 0.6
Temporal Lobe	27.90 ± 0.8	28.40 ± 0.4	28.30 ± 0.8	29.20 ± 0.4	29.00 ± 0.3	28.90 ± 1.1
Parietel Lobe	24.20 ± 0.4	24.60 ± 0.4	24.90 ± 0.5	26.10 ± 0.6	27.20 ± 0.7	26.20 ± 0.6
Occipital Lobe	27.10 ± 0.3	27.50 ± 0.2	28.00 ± 0.3	28.40 ± 0.9	29.20 ± 0.5	28.90 ± 0.5
Frontal Lobe	25.40 ± 0.4	25.90 ± 0.2	26.50 ± 0.5	26.50 ± 0.4	26.80 ± 0.3	26.80 ± 0.3
Caudate Nucleus	28.20 ± 0.4	27.70 ± 0.4	26.80 ± 1.0	28.60 ± 0.4	28.20 ± 0.4	28.30 ± 0.9
Globus Pallidus	27.30 ± 0.7	28.40 ± 0.5	27.80 ± 0.6	28.80 ± 0.9	28.40 ± 0.8	28.10 ± 1.3
Putamen	28.20 ± 0.3	27.40 ± 0.5	28.70 ± 0.3	29.10 ± 0.4	28.00 ± 0.6	27.80 ± 0.6
Thallamus	28.90 ± 0.7	28.60 ± 0.4	29.00 ± 0.3	29.90 ± 0.6	29.90 ± 0.3	29.40 ± 0.4

pared with the central white matter of the different lobes ($P < .01$). This was followed by the splenium, the central centrum semiovale, and the superior frontooccipital fasciculus, because of the presence of a large number of heavily myelinated white matter fibers in these structures. The temporal and the occipital lobes showed a slightly but statistically insignificant higher percent magnetization transfer when compared with the frontal lobes. The anterior commisure and the fornix had comparable percent magnetization transfers (Table 1).

Gray Matter

There was no statistical difference between the percent magnetization transfer of the gray matter in cerebellum and the temporal, parietel, occipital, and frontal lobes across all the age categories. The range of percent magnetization transfer of gray matter (24% to 29%; mean, 28% ± 2%) was lower than that of the white matter. The thalamus had the highest percent magnetization transfer (30% ± 0.5%) of any gray matter structure in the brain, which reflects the presence of myelinated white matter fibers. The caudate nucleus, globus pallidus, and putamen had similar percent magnetization transfer (28% ± 0.6%) for all age groups, which was statistically not significant compared with the thalamus (Table 2).

Discussion

With, MR, a variety of tissue contrast is obtainable by manipulating the variable parameters: T1-weighted, proton-density, and T2-weighted, flow and gradient-recalled echoes. Magnetization transfer is a method of determining the contribution of macromolecular protein cell wall protons to the MR signal. In this study we have explored the use of magnetization transfer in nondiseased, normal, intracranial structures. We sought to assess the variability of magnetization transfer in normal structures of the cranium and to see whether there was a variability in different adult age groups.

Magnetization transfer, which is derived from a saturation transfer technique, was described by Forsen and Hoffman (36). Subsequently, Wolff and Balaban in 1989 (2) demonstrated that the topology of water-macromolecular proton magnetization transfer can be determined by using MR imaging coupled with a saturation transfer technique. In their experiments, the restricted hydrogen magnetization was selectively irradiated using a power radio-frequency field off-resonance from the H_f. This results in a selective saturation of H_r magnetization. The H_r saturation is then transferred to the coupled H_f spins via the magnetization transfer process. Because the magnetization is transferred, the process is called *saturation transfer*. Koenig (37) has postulated that the primary magnetization transfer pathway in white matter is cross-relaxation between the cholesterol of myelin and surrounding water.

The percent magnetization transfer described in this study is equivalent to the magnetization transfer ratios calculated by other workers (22, 25): percent magnetization transfer or magnetization transfer ratio = signal of the region of interest (without magnetization transfer saturation) − signal of the region of interest (with magnetization transfer saturation)/signal of the region of interest (without magnetization transfer saturation). The percent magnetization transfer is a measure of the degree of signal suppression of a given tissue compared with the conventional T1-weighted sequences. On T1-

weighted images there was a qualitative difference in the appearance of the white and gray matter between the T1-weighted magnetization transfer and conventional T1-weighted spin-echo images. The MR signal from all brain structures was uniformly decreased on T1-weighted magnetization transfer compared with the T1-weighted images (Fig 1B). Moreover, even though all brain signal was uniformly decreased, the white matter was more suppressed than the gray matter (Fig 1). Correspondingly, the white matter had the higher percent magnetization transfer because of the greater degree of signal suppression on magnetization transfer saturation (Table 1). As a result of this differential saturation, gray matter of the thalamus, putamen, caudate, and globus pallidus (Fig 1) was rendered more intense than white matter and became conspicuous when the magnetization transfer pulse was applied.

In the current study, the highest percent magnetization transfer was found in the genu of the corpus callosum, followed by the splenium, centrum semiovale, and superior frontooccipital fasciculus. The ranges of percent magnetization transfer in the periventricular, deep, and subcortical white matter for the different lobes of the cerebrum were similar, and the differences were not statistically significant. There was also no significant variation in these measurements across the different age groups up to age 80 years (Table 1).

Among the gray matter structures, the thalamus had the highest percent magnetization transfer of any gray matter structure (cortical or deep periventricular) (Table 2). The thalamus appeared lower in signal on the magnetization transfer–saturated image (Fig 1) compared with the cortex or the basal ganglia, indicating a higher degree of suppression and a higher percent magnetization transfer. The value of percent magnetization transfer of the caudate and the putamen in our study was higher than the figures published by Mathews et al (25).

The cause of the differential saturation is not precisely known for the differences in percent magnetization transfer between white matter and gray matter. The degree of myelination, cerebroglycosides, phosphatidylcholine, and cholesterol in the white matter may all play an important role (38). Iron deposition and density of neurons have also been postulated (32). The higher magnetization transfer found in the genu and the splenium of the corpus callosum can be correlated histologically to the presence of a large number (300 million) of heavily myelinated white matter fibers in these structures (39). The higher thalamic percent magnetization transfer may also be related to the presence of myelinated afferent and efferent fibers entering and leaving the thalamus because of its various connections (40, 41).

In comparing our extensive white and gray matter measurements with previously published reports (8, 9), the percent magnetization transfer (magnetization transfer ratio) of the white matter in the centrum semiovale is similar and comparable to that published by authors of another study, that is, approximately 39% to 41%. These workers used an off-resonance magnetization transfer pulse that, compared with the on-resonance pulse used in this study, made normal white matter measurements in patients with metastatic lesions of the brain. The percent magnetization transfer in both their and our study is higher than that published by Mathews et al (25), who derived percent magnetization transfer (magnetization transfer ratios) from the proton-density and the T2-weighted sequences compared with the T1-weighted sequences. These differences may be related to the pulse design, scanning parameters, and the degree of power deposition and the type of MR imager, all of which affect the tissue saturation.

In conclusion, this study defines the percent magnetization transfer of normal gray and white matter of the brain. These data suggest that no significant change in percent magnetization transfer occurs as a result of aging. These data provide a quantitative baseline for percent magnetization transfer measurements.

References

1. Koenig SH, Brown RD, Ugolini R. A unified view of relaxation in protein solutions and tissue, including hydration and magnetization transfer. *Magn Reson Med* 1993;29:77–83
2. Wolff SD, Balaban RS. Magnetization transfer contrast (MTC) and tissue water proton relaxation in vivo. *Magn Reson Med* 1989;10:135–144
3. Ceckler TL, Balaban RS. Tritium-proton magnetization transfer as a probe of cross relaxation in acqueous lipid bilayer suspensions. *J Magn Reson* 1991;93:572–588
4. Balaban RS, Ceckler TL. Magnetization transfer contrast in magnetic resonance imaging. *Magn Reson Q* 1992;8:116–137
5. Kurki TJI, Neimi PT, Lundbom N. Gadolinium-enhanced magnetization transfer contrast imaging of intracranial tumors. *J Magn Reson Imaging* 1992;2:401–406

6. Neimi PT, Kurki TJI, Lundbom N, Karmano M. Magnetization transfer contrast in Gd-DTPA imaging of brain tumors. *Invest Radiol* 1991;26:S248–S249
7. Tanttu R, Sepponen E, Lipton MJ, Kuusela T. Synergistic enhancement of MRI with Gd-DTPA and magnetization transfer. *J Comput Assist Tomogr* 1992;16:19–24
8. Finelli DA, Hurst GC, Gullapali RP, et al. Improved contrast of enhancing brain lesions on post-gadolinium T1-weighted spin-echo images with use of magnetixzation transfer. *Radiology* 1994; 190:553–559
9. Boorstein JM, Wong KT, Grossman RI, et al. Metastatic lesions of the brain: imaging with magnetization transfer. *Radiology* 1994; 191:799–803
10. Yueng HN, Aisen A. Magnetization transfer contrast with periodic pulse saturation. *Radiology* 1992;183:209–214
11. Lundbom N. Determination of magnetization transfer tissue contrast: an MR study of brain tumors. *AJR Am J Roentgenol* 1992; 159:1279–1285
12. Kurki T, Neimi P, Valtonen S. MR of intracranial tumors: combined use of gadolinium and magnetization transfer. *AJNR Am J Neuroradiol* 1994;15:1727–1736
13. Mehta RC, Pike GB, Haros SP, Enzmann DE. Central nervous system tumor, infection and infarction: detection with gadolinium-enhanced magnetization transfer MR imaging. *Radiology* 1995; 195:41–47
14. Li W, Tkach JA, Haacke EM, Masaryk TJ. Intracranial MR angiography: application of magnetization transfer contrast and fat saturation to short gradient-echo, velocity compensated sequences. *Radiology* 1993;186:753–761
15. Atkinson D, Brant-Zawadski M, Gillan G, et al. Improved MR angigraphy: magnetization transfer suppression with variable flip angle excitation and increased resolution. *Radiology* 1994;190: 890–894
16. Edelman RR, Ahn SS, Chien D, et al. Improved time of flight MR angiography with magnetization transfer contrast. *Radiology* 1992;184:395–399
17. Tkach JA, Lin W, Duda JJ, Haacke EM, Masaryk TJ. Optimizing three-dimensional time of flight MR angiography with variable repitition time. *Radiology* 1994;191:805–811
18. Pike GB, Hu BS, Glover GH, Enzmann DR. Magnetization transfer time of flight magnetic resonance angiography. *Magn Reson Med* 1992;25:372–379
19. Tkach JA, Ruggieri PM, Ross JS, Modic MT, Dillinger JJ, Masaryk TJ. Pulse sequence strategies for vascular contrast in time of flight carotid MR angiography. *J Magn Reson Imaging* 1993;3:811–820
20. Wolff SD, Eng J, Balaban RS. MTC: method of improving contrast in gradient recalled echo images. *Radiology* 1991;179:133–137
21. Dixon WT. Use of magnetization transfer contrast in gradient-recalled-echo images. *Radiology* 1991;179:15–16
22. Dousset V, Grossman RJ, Ramer KN, et al. Experimental allergic encephalomyelitis and multiple sclerosis: lesion characterization with magnetization transfer imaging. *Radiology* 1992;182:483–491
23. Tomiak MM, Rosenblum JD, Prager JM, Metz CE. Magnetization transfer: a potential method to determine the age of multiple sclerosis lesions. *AJNR Am J Neuroradiol* 1994;15:1569–1574
24. Prager JM, Rosenblum JD, Huddle DC, Diamond PK, Metz CE. The magnetization transfer effect in cerebral infarction. *AJNR Am J Neuroradiol* 1994;15:1497–1500
25. Mathews VP, King JC, Elster AD, et al. Cerebral infarctions: effects of dose and magnetization transfer contrast at gadolinium enhanced MR imaging. *Radiology* 1994;190:547–552
26. Ordidge RJ, Helperin JA, Knight RA, Qing Z, Welch KMA. Investigation of cerebral ischemia using magnetization transfer contrast (MTC) MR imaging. *Magn Reson Imaging* 1991;9:895–902
27. Finelli DA, Hurst GC, Karamon DA, et al. Use of magnetization transfer for improved contrast on gradient-echo MR images of cervical spine. *Radiology* 1994;193:165–171
28. Wolff SD, Chesnick S, Frank JA, et al. Magnetization transfer contrast: MR imaging of the knee. *Radiology* 1991;179:623–628
29. Balaban RS, Chesnick S, Hedges K, et al. Magnetization transfer contrast in MR imaging of the heart. *Radiology* 1991;180:671–675
30. Prasad RV, Burstein D, Edelman RR. MRI evaluation of myocardial perfusion without a contrast agent using magnetization transfer. *Magn Reson Med* 1993;30:267–270
31. Lexa FJ, Grossman RI, Rosenquist AC. MR of Wallerian degeneration in feline visual system: characterization by magnetization transfer rate with histopathologic correlation. *AJNR Am J Neuroradiol* 1994;15:201–212
32. Elster AD, King JC, Mathews VP, et al. Cranial tissues: appearance at gadolinium-enhanced and nonenhanced MR imaging with magnetization transfer contrast. *Radiology* 1994;190:541–546
33. Pike GB, Glover GH, Hu BS, Enzmann DR. Pulsed magnetization transfer spin-echo imaging. *J Magn Reson Imaging* 1993;3:531–539
34. Hu BS, Conolly SM, Wright GA, Nishimura DG, Macovski A. Pulsed saturation transfer contrast. *Magn Reson Med* 1992;26: 231–240
35. Bracewell R. *The Fourier Transform and Its Application*. New York: McGraw-Hill, 1965;5:5–67
36. Forsen S, Hoffman RA. Study of moderately rapid chemical exchange reactions by means of nuclear magnetic double resonance. *J Chem Phys* 1963;39:2892–2901
37. Koenig SH. Cholesterol of myelin is the determinant of gray-white contrast in MRI of brain. *Magn Reson Med* 1991;20:285–291
38. Kucharczyk W, MacDonald PM, Stanisz GJ, et al. Relaxivity and magnetization transfer of white matter at MR imaging: importance of cerebrosides and pH. *Radiology* 1994;192:521–529
39. Barr ML, Kierna JA, eds. *The Human Nervous System: An Anatomical Viewpoint*. 5th ed. Philadelphia: JB Lippincott, 1988: 244–258
40. Barr ML, Kierna JA, eds. *The Human Nervous System: An Anatomical Viewpoint*. 5th ed. Philadelphia: JB Lippincott, 1988: 178–206
41. Jones EG. *The Thalamus*. New York: Plenum Press, 1985